



Relaxation of Process-Induced Stresses in Composite Parts – Mixed Experimental-Numerical Approach

Anna GALIŃSKA

Institute of Aviation

Al. Krakowska 11/114, 02-256 Warsaw, Poland
e-mail: anna.galinska@ilot.edu.pl

The main source of the process-induced deformations are stresses which occur in composite parts during cure. Those stresses cause unexpected reduction of the part strength which may bring about catastrophic consequences. The measurements of the process-induced stresses in composite parts are very difficult, so the problem has been neglected so far. Therefore, in the scope of the present work an attempt is made to evaluate the stresses in composite parts made of carbon/epoxy unidirectional prepreg by a numerical simulation. The results of the simulation are verified by the comparison of the calculated and measured deformations of a composite part. Since the composite materials exhibit viscoelastic behaviour, some of the process-induced stresses in composite parts may be relaxed during exploitation of the part, which may lead to the decrease of the undesired process-induced stresses. Therefore, a user defined viscoelastic-orthotropic material model was developed in order to take into account the stress relaxation. Such an approach allowed to evaluate the process-induced stress level in composite parts during exploitation without difficult and time-consuming experiments.

Key words: process-induced stresses; carbon-epoxy composite; stress relaxation; Finite Element Method.

1. INTRODUCTION

The process-induced deformations of composite parts is a well-recognized problem which often prevents engineers from manufacturing the parts within the dimensional tolerance. The deformations are caused by the residual stresses which occur in the composite material as the result of the cure process. The stresses are caused mainly by the mismatch between the coefficients of thermal expansion, chemical shrinkage of the resin and interaction with the tool. In the following work the two former factors will be taken into account, since experiments conducted in the scope of the previous work has shown that their influence on the process-induced deformations is most significant [1]. The process-induced

deformations cause many unfavourable effects such as inaccurate geometry, difficulties in the part assembly and decrease of the strength of the structure due to residual and assembly stresses. The last phenomenon is the one that is of interest in the following work. The residual stresses resulting from the cure cycle are partially dissipated after demoulding of a composite part due to the deformation of the part. However, part of the stresses is still present in the composite and after assembly of the deformed part with the rest of the structure additional assembly stresses rise in it (Fig. 1).

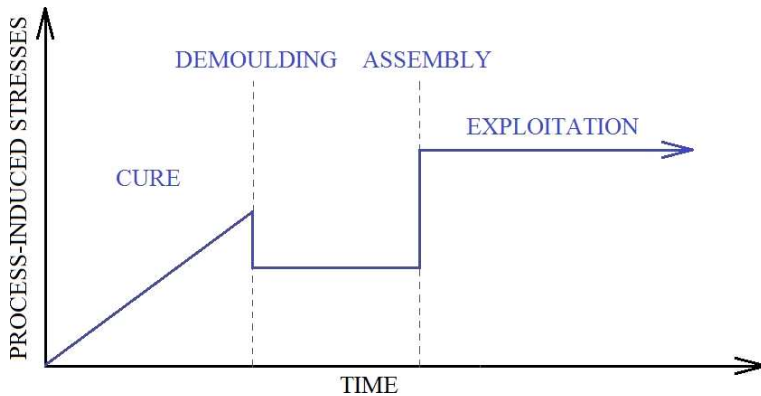


FIG. 1. Process-induced stresses development during stages of composite part 'life'.

Combined residual and assembly stresses may constitute significant part of the composite material strength. As those stresses originate from the manufacturing process, in the present paper they will be referred to as the process-induced stresses. Since the process-induced stresses are usually not taken into account in the stress analysis of the part, they may cause its unexpected failure.

The process-induced stresses of composite parts are very difficult and tedious to measure. They can be measured by placing strain sensors, e.g. fibre Bragg grating (FBG) sensors or strain gauges [2–4] between composite plies. However, since the FBG sensors has large diameter (125 μm to 230 μm) compared to the carbon fibres, embedding the optical fibre perpendicularly to the direction of the reinforcement fibres can result in appearance of characteristic 'eye' patterns or 'pockets' within the resin, which act as defect centres in the composite part that could ultimately lead to premature failure in the form of delamination [5, 6]. Such a failure could disturb the measurements significantly. Moreover, as the gauge separates fibres, resin rich regions may appear along it, which may cause artificial overstatement of the process-induced stresses, since the resin rich regions shrinks more than intact composite. Strain gauges may cause similar problems as FBG sensors or even more severe problems with defects due to their considerable area

of a few square millimetres. A straightforward technique to measure process-induced stresses is called successive grooving technique (SGT). It consists in successive cutting of the material through the thickness and relating resulting deformations to the magnitude of the process-induced stresses released by the cutting [7]. Both above techniques require manufacturing additional composite parts in addition to the required ones in every manufacturing process, which significantly increases costs and time of the process.

Since the composite material is known to have viscoelastic properties, the process-induced stresses may decrease in time as the result of the stress relaxation. However, the stress relaxation is extremely difficult to measure, because of the long time in which the measurements have to be carried out. An attempt to measure the process-induced stress relaxation with the use of the techniques cited above would complicate the measurements even further. Therefore, the problem of the decrease of composite parts strength due to the residual and assembly stresses has been neglected in the strength evaluation of the composite parts so far. In the present work a combination of experimental and numerical methods is employed to evaluate the process-induced stresses and their relaxation in a composite part. The first part of the work consists in the measurements of the stress relaxation of cured composite specimens with the use of DMA (dynamic mechanical analyser). The measurements allow to obtain relaxation curves for short times, so in order to obtain the curves for longer times, the time-temperature superposition principle has to be used. In the second part of the work the relaxation curves are used in the FEM (finite element method) analysis of a C-sectioned spar in order to assess the level of the process-induced stresses in the part after demoulding, after assembly and as the stress relaxation proceeds. The results of the analysis allows to supply the awkward measurements of process-induced stresses in composite parts in order to assess the process-induced stresses and the resulting part strength.

There have been many models, both elastic and viscoelastic, used to evaluate the process-induced stresses (mainly residual) in composite parts and the process-induced deformations resulting from them. There are two main types of models used for such calculations: analytical and numerical. Even though simple two-dimensional analytical models are successfully used to calculate the process-induced deformations of simple composite parts, the full description of the stresses in a composite part requires a three-dimensional model, because one- and two-dimensional models of stress distribution would neglect the three-dimensional effects. The three-dimensional model has to be developed with the use of numerical procedure, because the analytical models are too simple to permit three-dimensional calculations. Therefore, in the present work a three-dimensional numerical model will be used to calculate the stresses

and deformations of a composite part. There have been several such models developed so far. DONG used an elastic three-dimensional model to predict the deformations of a composite structure [8, 9]. Only the influence of the thermal and chemical shrinkage was taken into account in this model. DING *et al.* used a user defined subroutine UMAT in FE software Abaqus in order to assess the thermal dependence of stresses in composite parts during curing [10, 11]. CLIFFORD *et al.* developed a viscoelastic numerical model with the use of Abaqus, which was used to calculate the deformations of a composite car floor panel and a C-sectioned element [12]. Since the commercial FE software does not usually have an opportunity to combine viscoelastic and orthotropic properties needed in such an analysis, a user defined viscoelastic-orthotropic material model was also used in this case. In this analysis three-dimensional brick elements were used to calculate the deformations. LI *et al.* used a similar model to calculate the deformations of a three-dimensional aerospace structure [13].

2. EXPERIMENTAL DETERMINATION OF RELAXATION MASTER CURVES

2.1. Material and process

All the experiments in the following sections were conducted for the unidirectional carbon/epoxy prepreg MTM-46/GF0103-38%RW. The cure process of this prepreg may be performed both in an autoclave and out-of-autoclave in an oven with the use of a vacuum bag (VBO). In this work, a VBO cure was used. The cure cycle consists of a 2°C/min ramp and 8 h dwell period in 80°C temperature followed by cooling.

2.2. DMA experiment

The stress relaxation behaviour is measured with the use of DMA. The specimens with dimensions approximately $50 \times 5 \times 5$ mm were cut from an unidirectional composite plate cured in the cycle described in Subsec. 2.1. The dynamic three-point-bending tests of the specimens was performed. During the tests the specimens were placed on the rigid supports in the DMA furnace and loaded by the driving shaft. As the temperature was raised during the tests it was controlled by the DMA temperature gauge. All the specimens were tested for several frequencies. As the reinforcement of the specimens was orientated perpendicularly to the plane of bending, the result of the tests were storage modulus $E'_y(\omega)$ and loss modulus $E''_y(\omega)$ in the y direction perpendicular to the fibres (Fig. 2).

The relaxation moduli $E(t)$ or $G(t)$ can be calculated on the basis of storage and loss moduli [14, 15]. Since for most epoxy systems the loss modulus is usually

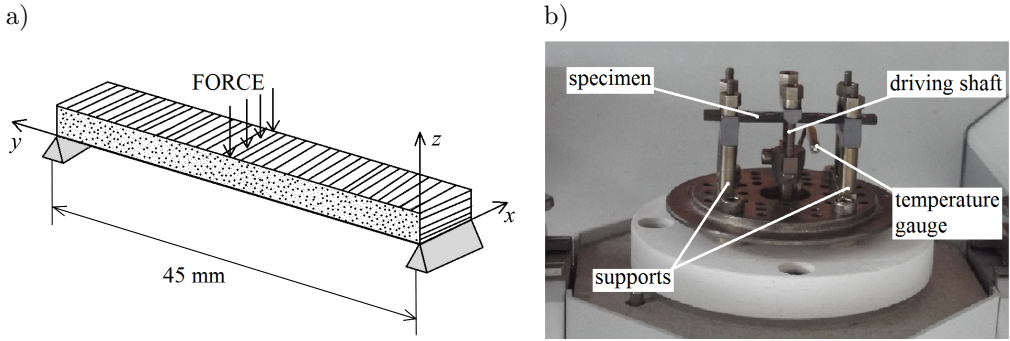


FIG. 2. DMA experiment: a) scheme of the experiment configuration; b) specimen in the DMA experimental stand configured for three-point-bending. The stand is covered by furnace during the tests.

much lower than the storage modulus, the relation between the dynamic and relaxation moduli can be simplified (Eq. (2.1)) [16–18]

$$(2.1) \quad G(t) = G' \left(\omega = \frac{1}{t} \right),$$

where the shear modulus G can be replaced by the modulus E . The three-point-bending dynamic tests were performed for various temperatures for each of the specimens. The glass transition temperature T_g of the composite cured in the same cure cycle was measured with the use of the DMA according to the standard ASTM D7028 [19] to be 70°C. As long as the material is below glass transition temperature, it is thermorheologically simple, which means that the time-temperature superposition principle can be applied to it. The principle consists in the assumption that the rheological behaviour of a material in higher temperature is equivalent to its behaviour for longer times [14, 20]. Since the relaxation functions are usually plotted against logarithmic axis, according to the time-temperature superposition the change of the temperature causes horizontal shift of the function. The shift factor $a_T(T)$ is dependent on the material and temperature. It can be described by Arrhenius or Williams, Landel and Ferry (WLF) equation. According to FERRY [14], in the case of polymer materials the second equations is usually used (Eq. (2.2))

$$(2.2) \quad \log a_T = - \frac{C_1 (T - T_{ref})}{C_2 + (T - T_{ref})},$$

where C_1 and C_2 are constants and T_{ref} is the reference temperature. FERRY proposed ‘universal’ constants for amorphous polymers: $T_{ref} = T_g$, $C_1 = 17.44$ and $C_2 = 51.6$. The curve which results from the horizontal shifts is called the master curve [20].

The DMA dynamic tests were performed on 8 specimens: each was tested in temperatures from 25°C to 70°C with frequencies ranging from 0.01 Hz to 10 Hz. The results of the tests against the frequency and the time are presented in Fig. 3.

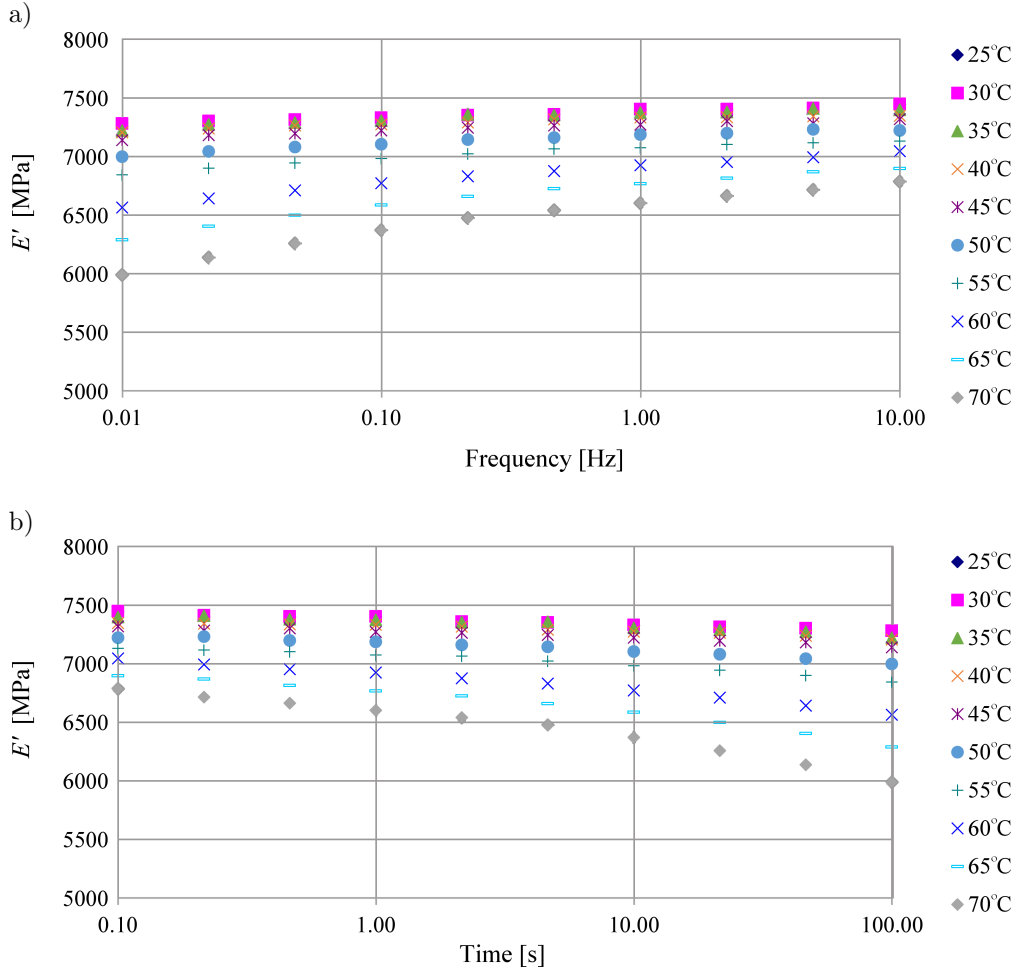


FIG. 3. Storage modulus E' in respect to: a) frequency and b) time.

Although the WLF shift factor is widely used in the analysis of the relaxation curves, in the following work factors found empirically are used, because those factors assured better alignment of the relaxation curves. An exemplary master curve obtained with the use of the empirical shift factors is presented in Fig. 4a. An average master curve was calculated after testing all 8 specimens (Fig. 4b). The maximum coefficient of variation for the master curve is equal to 4.2%.

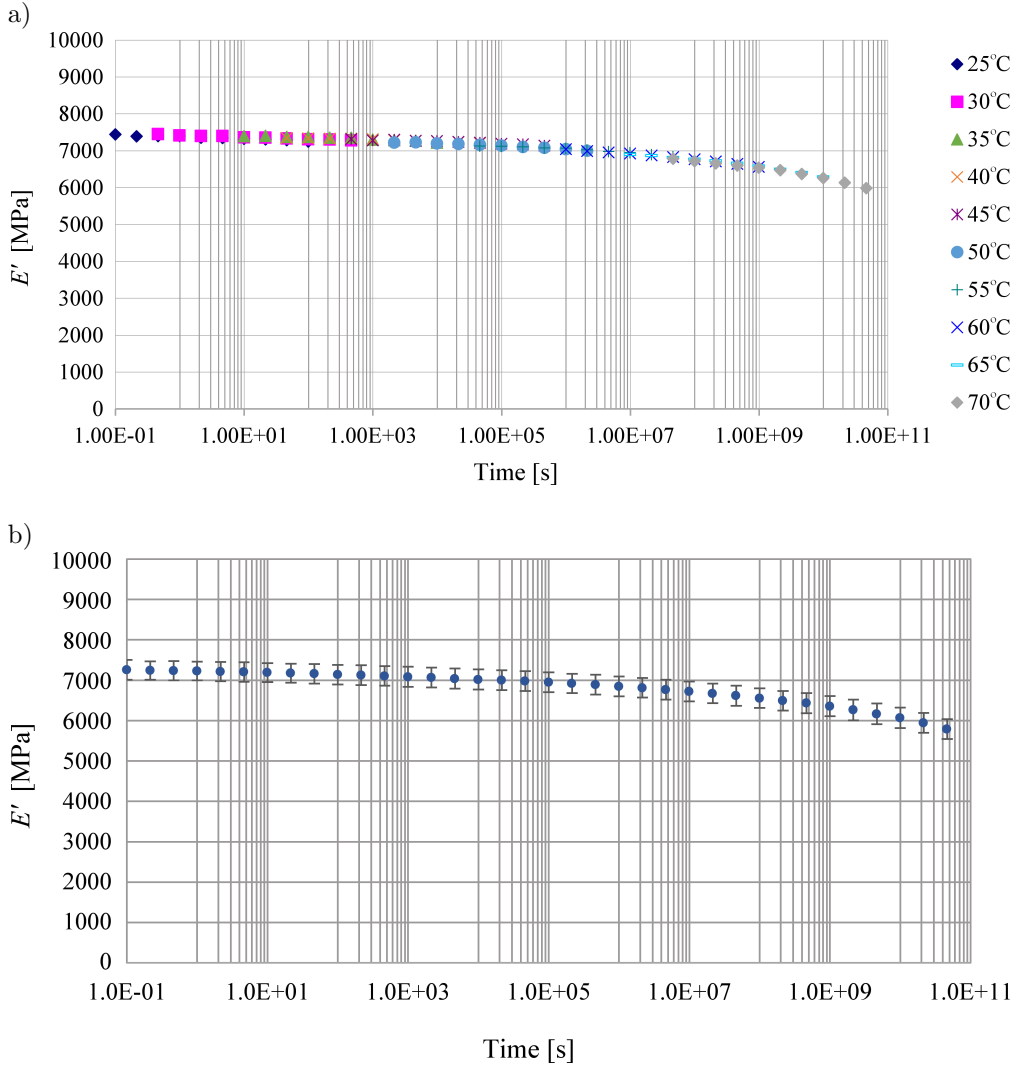


FIG. 4. a) Exemplary relaxation master curve for $T_{ref} = 25^\circ\text{C}$, b) average master curve for $T_{ref} = 25^\circ\text{C}$ with standard deviation for each data point.

3. PROCESS-INDUCED DEFORMATIONS

There are many sources of residual stresses and process induced deformations listed in literature. One of the most important mechanisms which contributes to the process-induced deformations is so-called spring-in, caused by inherent coupling of anisotropy and geometry in curved composite parts [21]. In fact it was found out that the spring-in is the only significant factor contributing to

the deformations of carbon-epoxy C-sectioned specimens cured VBO [1]. The spring-in is caused by different coefficients of thermal expansion (CTEs) in direction perpendicular and parallel to the fibres and by chemical shrinkage of the resin [22]. The coefficient of thermal expansion in the direction of fibres is much lower than perpendicular to them, because the carbon fibres have very low or even negative longitudinal CTE in comparison to polymer resins: the CTE of carbon fibres is reported to be $-0.4 \cdot 10^{-6} \text{ 1/}^\circ\text{C}$ [8] or $-0.9 \cdot 10^{-6} \text{ 1/}^\circ\text{C}$ [23], while the CTEs of epoxy resin are equal to $71 \cdot 10^{-6} \text{ 1/}^\circ\text{C}$ above and $210 \cdot 10^{-6} \text{ 1/}^\circ\text{C}$ below the T_g [24]. The CTE in transverse fibre directions is also higher than in longitudinal direction: $18 \cdot 10^{-6} \text{ 1/}^\circ\text{C}$ [8] and $7.2 \cdot 10^{-6} \text{ 1/}^\circ\text{C}$ [23]. The combined coefficient of thermal expansion is then much lower in the composite ply plane along the fibres than in the through-the-thickness direction. Therefore, as a curved composite part cures, its thickness decreases more rapidly than its circumferential dimensions. As the result of the thickness reduction the outer radius of the part tends to shorten and the inner to elongate. Since the reinforcing carbon fibres are stiff and do not change their dimensions easily, a bending moment occurs, which decreases the enclosed angle of the cured composite part (Fig. 5).

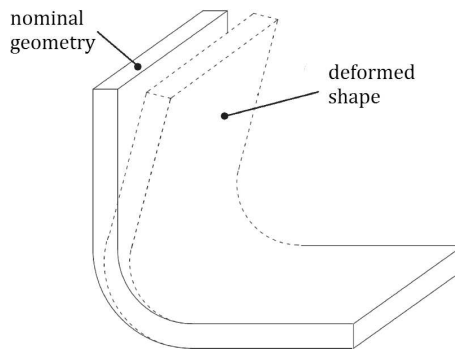


FIG. 5. Spring-in mechanism.

Chemical shrinkage of the resin which takes place during polymerization has a similar effect on the spring-in deformation as the thermal contraction of the resin. It takes place only in the directions perpendicular to the fibres, since only in those directions it is not hindered by stiff fibres. Therefore, the chemical shrinkage increases the spring-in deformation.

3.1. Experiment

The composite element for which numerical analysis was performed is a fragment of a C-sectioned spar. Its geometry and ply orientation is shown in Fig. 6. The specimens were manufactured from the same material, for which viscoelastic

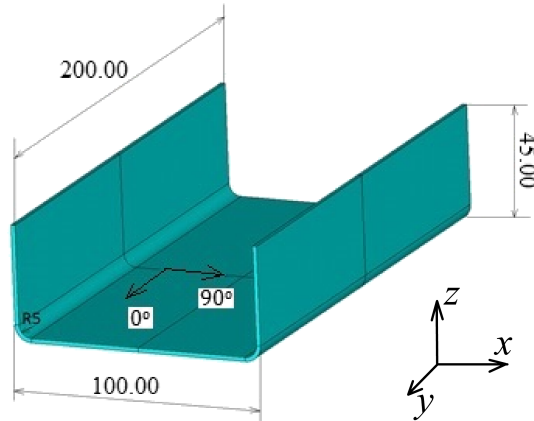


FIG. 6. C-sectioned specimen.

material characterization was performed in Sec. 2. There were 6 such specimens manufactured in the cure cycle described in Subsec. 2.1. The lay-up of the specimens is $[0^\circ/90^\circ/90^\circ/90^\circ/90^\circ/0^\circ]_S$. This lay-up is not a very common choice for C-sectioned elements which are often used as spars. The lay-up with large percentage of $-45^\circ/45^\circ$ oriented plies would be preferable in the case of such parts. However, in this work $0^\circ/90^\circ$ lay-up was chosen for the sake of the simplicity of the results interpretation and the specimen manufacturing. The specimens were cured on a convex aluminium tool.

The deformations of the C-sectioned specimens were measured with the use of a coordinate measuring machine (CMM) DEA GLOBAL. The spring-in deformation of each specimen was measured in the middle cross-section of the specimen, so the deformation of two angles was obtained for each specimen. The tool, on which the specimens were manufactured was also measured in the corresponding section. The deformation for each specimen was defined as the difference between the angles of the tool and the corresponding angles of the specimen. The average measured spring-in angle is equal to 1.00° with standard deviation of 15.3%. The same results were used in the previous work concerning different models used to predict the process-induced deformations of composite parts [25].

4. NUMERICAL CALCULATIONS

The following section starts with the description and validation of a linear elastic numerical model which allows to calculate the process-induced deformations and stresses of composite parts. Then this model is expanded to the viscoelastic model which allows to calculate the process-induced stresses in any moment of the composite part ‘life’.

4.1. Validation of linear elastic numerical model

The numerical model used to calculate process-induced stresses and deformations of the C-sectioned specimens was developed in Ansys FEM software. 8-node brick elements SOLID185 were used to model the composite part. Seven layers of elements were used in the through-the-thickness direction to model lay-up of the part. The model consists of 65 800 elements. The directions of orthotropic plies were set by local element coordinate systems. The tool was not modelled at all in the analysis which uses the linear elastic material model, since the analysis takes into account only the cooling of the part. Due to the double symmetry of the part, only a quarter of it was modelled. The model along with its boundary conditions is shown in Fig. 7a. The assigned thermal load ΔT was equal to -60°C , since the specimen after cure is cooled from 80°C to the room temperature.

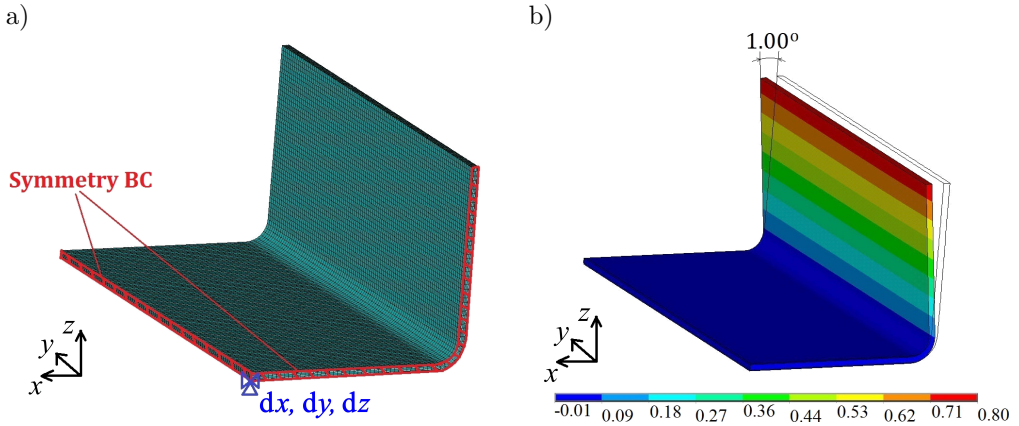


FIG. 7. a) Numerical model – dx , dy and dz denote displacements fixed in respectively x , y and z directions, b) spring-in deformation calculated with the use of the numerical model.

Nine mechanical properties of the composite materials are used in the FEM model for the linear elastic calculations in directions x , y and z shown in Fig. 2. The values of these properties are partially acquired from the manufacturer's data sheets and partially are assumed [25]:

$$\begin{aligned}
 E_x^* &= 128\,242 \text{ MPa}, & E_y &= E_z = 7260 \text{ MPa}, \\
 \nu_{xy}^* &= \nu_{xz}^* = 0.288, & \nu_{yz} &= 0.3, \\
 G_{xy}^* &= G_{xz}^* = 4282 \text{ MPa}, & G_{yz} &= 3368 \text{ MPa}.
 \end{aligned}$$

The values acquired from datasheet are denoted by *. The discussion of the reliability of the assumed values is carried out in the previous work [25].

Although the $E_y = E_z$ value is available in the manufacturer's datasheets (8756 MPa), the value of this property for linear elastic material model was taken from the experiments in Sec. 2 for the lowest relaxation time. It is lower than the value presented in the manufacturer's datasheet, but the value obtained from the DMA tests ought to be used, because the further part of the calculations concerns the viscoelastic behaviour of the material and the DMA relaxation moduli will be used in them.

The deformation modelling approach was similar to the one used by RADFORD and RENNICK and DONG [8, 9, 22], where only thermal and chemical shrinkage were considered as the factors contributing to the process-induced deformations of the composite parts. These factors were measured in the previous works [1, 25]. Both measured thermal and chemical shrinkage values are implemented in the numerical model as coefficients of thermal expansion (CTE). The CTEs of the composite in directions parallel and perpendicular to the reinforcing fibres were measured with the use of a dilatometer. Chemical shrinkage was measured as a through-the-thickness strain of the material during cure. The in-plane chemical strain along the reinforcing fibres was neglected, since it is hindered by the fibres which are stiff and are not subjected to chemical changes during cure. The in-plane chemical strain in direction perpendicular to the fibres is identical to the through-the-thickness strain in the case of unidirectional composite. Substitutive CTEs used in the numerical model instead of thermal and chemical shrinkage are equal to [25]:

$$\alpha_x = 0.0000013 \text{ } 1/^{\circ}\text{C}, \quad \alpha_y = \alpha_z = 0.0001553 \text{ } 1/^{\circ}\text{C}.$$

The spring-in angle was calculated as the change of angle of the specimen flange (Fig. 7b). The calculated spring-in angle is equal to 1.00° . This indicates that the numerical model results are valid, because this value is identical to the measured spring-in angle.

4.2. Relaxation of residual stresses in composite parts

As the process-induced deformations calculated with the use of the linear elastic numerical model agrees with the real deformations, it is assumed that the process-induced stresses are also calculated correctly in this model. Therefore, on the basis of this model a viscoelastic model, which allows to take into account the stress relaxation, was developed by changing the material model from linear elastic to viscoelastic. Since none of the commercial FEM software, including Ansys, provides opportunity to combine orthotropic and viscoelastic properties for one material, a user defined material has to be used in order to model macroscopic viscoelastic behaviour of composite materials. An approach used earlier by BARBERO [26] was employed in order to assign viscoelastic properties

to the orthotropic material by a USERMAT procedure. Instead of the constant value of $E_y = E_z$, a Prony series, which is often used to describe mathematically relaxation curves [23, 27], was used. The Prony series used in Ansys to model isotropic viscoelastic material is described by the Eq. (4.1):

$$(4.1) \quad E(t) = A_0^2 + \sum_{i=1}^N A_i^2 e^{-\frac{t}{\tau_i}},$$

where A_0 , A_i and τ_i are coefficients found by the nonlinear regression method in order to fit the series to the experimental curve. The same equation was used to define the coefficients of 6-element Prony series fitted to the master curve obtained from the DMA experiments in Sec. 2 (Fig. 4b). The master curve covers time range from 10^{-1} s to 10^{11} s, which exceeds the time of exploitation of any composite product, so the Prony series was fitted only for its useful range (10^{-1} s – 10^8 s). The FEM model used for the viscoelastic analysis was basically the same as the one used in previous section for the elastic analysis, but the material model was changed from linear orthotropic to viscoelastic orthotropic defined by the USERMAT subroutine. Process-induced stresses for four points in the composite part history were calculated with the use of the numerical model:

- 1) after cooling of the part, but before demoulding ($t = 10^4$ s),
- 2) just after the demoulding ($t = 10^4 + 1$ s),
- 3) just after assembly ($t = 10^6$ s),
- 4) after over three years from the assembly ($t = 10^8$ s).

In order to model the first step of the analysis, the process-induced stresses before the demoulding, the influence of the tool had to be modelled to provide the correct boundary conditions. The influence was modelled by adding fixed displacements on the inner areas of the model in the x , y , and z directions to the boundary conditions used in linear elastic analysis (Fig. 8a). In the second step, as the composite part was demoulded, the boundary conditions were the same as in the case of the linear elastic analysis (Fig. 7a). In the last two steps the fixed displacement in x direction was added on the edge of the C-sectioned specimen in order to model its assembly with the rest of the structure by adhesive bounding or riveting (Fig. 8b).

The first step of the analysis was performed for time 10^4 s, which models the fact that the composite part may be kept in the tool some time before demoulding. The second step, as it models demoulding, is performed for time $10^4 + 1$ s. Then it is assumed that the part is assembled several days after manufacturing (10^6 s). The final step of the analysis is performed for the time of over three years of exploitation of the assembled part (10^8 s). This time points were chosen in order to imitate an exemplary composite part history. The time

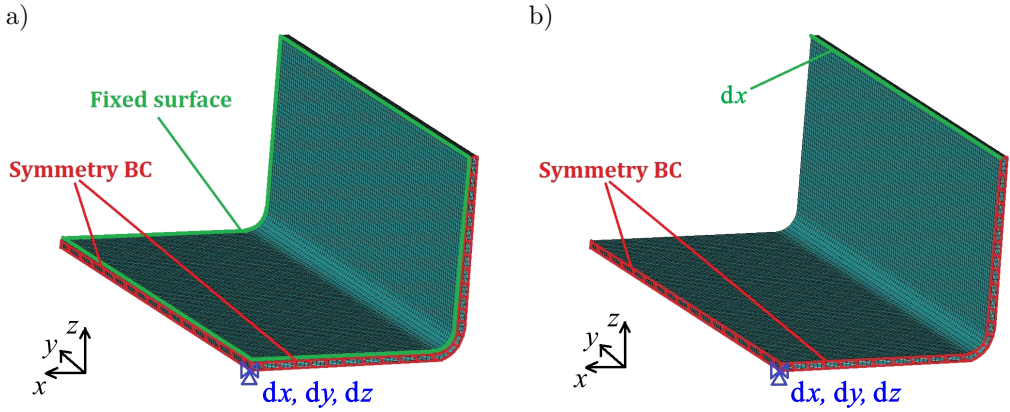


FIG. 8. Boundary conditions used in: a) step 1, b) step 3 and 4 of the analysis; dx , dy and dz denote fixed displacements in respectively x , y and z directions.

values, however, can be changed at will and can imitate any composite part history. The process-induced stresses calculated at the end of the each step are shown in the Figs. 9–12. The figures show circumferential stresses in the part corner, since those stresses are the main result of the spring-in deformation. Only the stresses in the specimen plane of symmetry are taken into account. The circumferential stresses are presented for each step separately for the 90° directed plies (fibres oriented across the C-sectioned specimen – see Fig. 6) and for 0° directed plies (fibres oriented along the C-sectioned specimen – see Fig. 6).

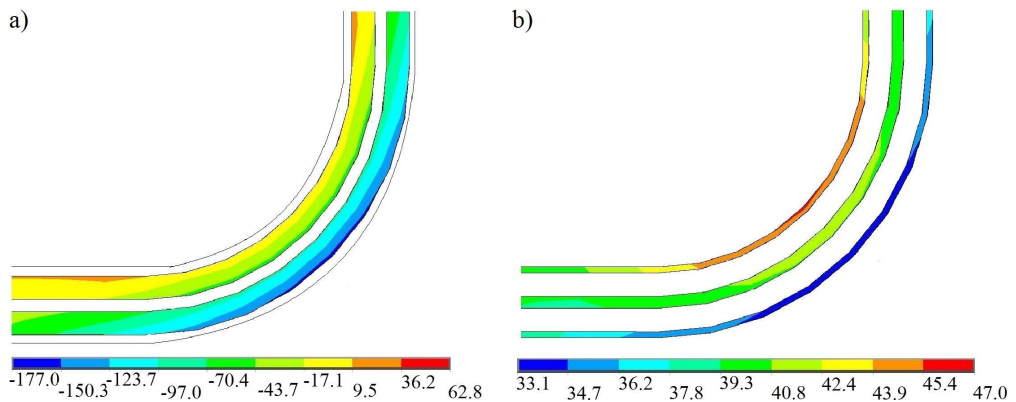


FIG. 9. Circumferential stresses [MPa] in C-sectioned specimen corner after 1st step: a) in 90° oriented plies, b) in 0° oriented plies.

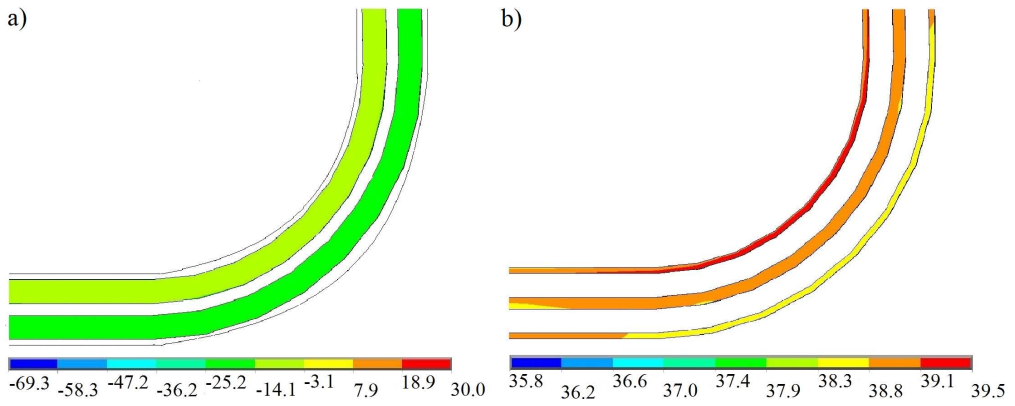


FIG. 10. Circumferential stresses [MPa] in C-sectioned specimen corner after 2nd step:
 a) in 90° oriented plies, b) in 0° oriented plies.

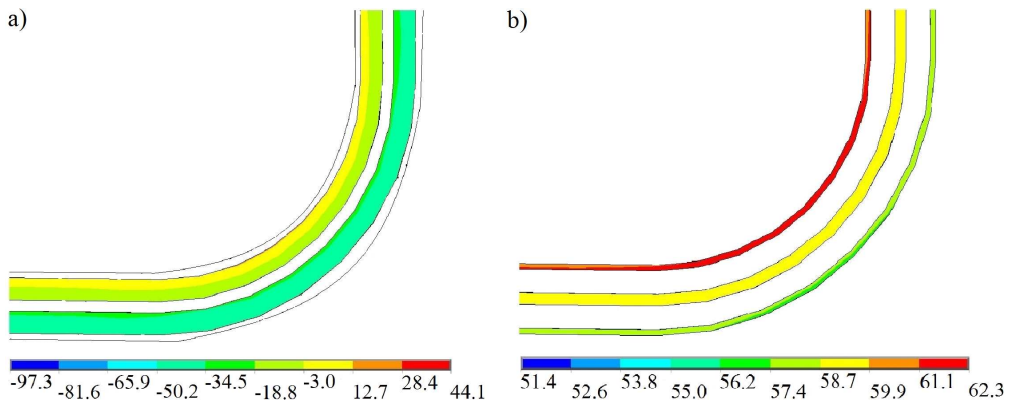


FIG. 11. Circumferential stresses [MPa] in C-sectioned specimen corner after 3rd step:
 a) in 90° oriented plies, b) in 0° oriented plies.

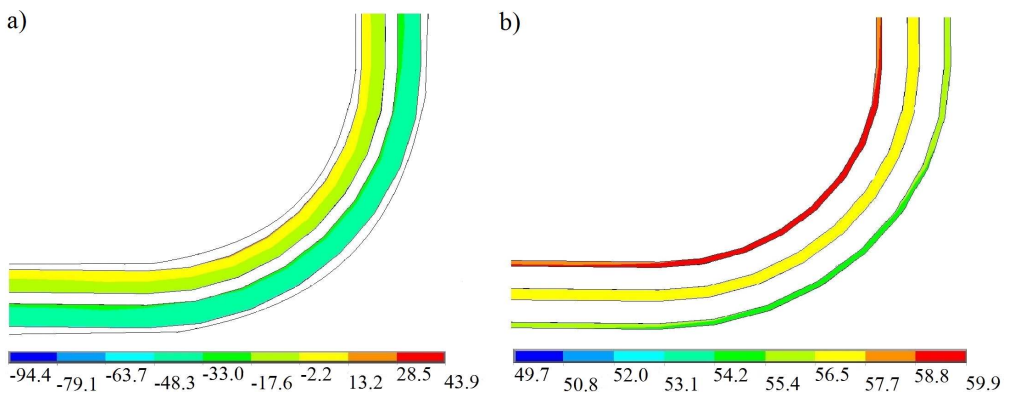


FIG. 12. Circumferential stresses [MPa] in C-sectioned specimen corner after 4th step:
 a) in 90° oriented plies, b) in 0° oriented plies.

In order to evaluate the significance of the calculated stresses they have to be compared to the strength of the composite material in question. The strength values for MTM-46/GF0103-38%RW material taken from the manufacturer's datasheet are presented in Table 1.

Table 1. Strength values of the composite materials.

	Strength [MPa]
Tension 90°	2017.06
Compression 90°	1286.56
Tension 0°	34.40
Compression 0°	197.88

It may be noticed on the basis of the results of the calculations (Figs. 9–12) that the main stresses in the 90° plies are compressive and in the 0° plies are tension-type. This is not surprising, since as the part is cooled, the plies contract as the result of the thermal and chemical shrinkage much more in the direction y perpendicular to the fibres, than in direction x along the fibres. This results in compressing of the 90° plies which have fibres oriented circumferentially by the 0° plies, which have fibres oriented along the part. On the other hand 90° plies tend to prevent contraction of the 0° plies causing rise of tension in them. Firstly, the stresses in 90° oriented plies will be considered. In the first step of the calculations the highest stresses are equal to -177 MPa in the outer plies. This stress constitutes almost 14% of the material strength, however, since the stress decreases rapidly to -25 MPa after demoulding in the second step, it does not pose a danger to the part strength. The stress after assembly increases to -50 MPa and hardly decreases owing to relaxation after three years. This stress constitutes about 4% of the part strength, which is not a significant part, however, in certain load cases, when the load is close to its ultimate value, they may contribute to an unexpected part failure. The stresses in the 0° plies do not change significantly over the steps of the analysis. The maximum stress in them is equal to 47 MPa, 40 MPa, 61 MPa and 60 MPa in the successive steps. All these values are higher than the tension strength of the 0° ply, which may lead to the plies cracking even without external load, in any of the manufacturing and exploitation stages. The resulting cracks may cause the decrease of the part strength and its failure. The last two steps of the analysis show that the decrease of the process-induced stresses due to the relaxation process is also hardly noticeable in the case of the 0° plies.

5. CONCLUSIONS

In the above work a mixed experimental-numerical approach has been used in order to evaluate the process-induced stresses in composite parts. Since

there is no simple experimental technique to measure those stresses, the presented approach seems to be a useful alternative for pure experiments. The experimental-numerical approach was employed to evaluate the process-induced stresses in a C-sectioned composite specimen. Two main conclusions may be drawn on the basis of the results:

The process-induced stresses may constitute a significant part of the composite part strength. Therefore, it is advisable to include the process-induced stress analysis, e.g. by experimental-numerical approach, to the strength analysis of the designed composite part.

The results of the experimental-numerical analysis indicate that the stress relaxation process, which is considered to decrease the process-induced stresses, has hardly any influence on their magnitude after three years of the composite part exploitation. It suggests that the relaxation of the process-induced stresses in the composite parts does not help to improve the part strength.

However, those conclusions are drawn on the basis of one relatively simple case study. Much wider range of cases should be considered in order to acknowledge their usefulness for all composite parts.

ACKNOWLEDGMENTS

This research was funded from the project ‘Development of the technology for testing the resistance to damage of aviation and space composite load bearing structures’ – TEBUK, No. POIG.01.01.02-14-017. The project is financially supported by European Regional Development Fund within the framework of Innovative Economy – National Cohesion Strategy.

REFERENCES

1. OSMEDA A., *Measurements of strain induced by chemical shrinkage in polimer composites*, Journal of Polymer Engineering, **36**: 431–440, 2016.
2. POTTER K., CAMPBELL M., WISNOM M., *Investigation of tool/part interaction effects in the manufacture of composite components*, Proceedings of the 14th International Conference on Composite Materials, San Diego, 2003.
3. MULLE M., COLLOMBET F., OLIVIER P., GRUNEVOLD Y-H., *Assessment of cure residual strains through the thickness of carbon-epoxy laminates using FBGs, Part I: Elementary specimen*, Composites: Part A, **40**, 94–104, 2009.
4. MULLE M., COLLOMBET F., OLIVIER P., ZITOUNE R., HUCHETTE C., LAURIN F., GRUNEVOLD Y-H., *Assessment of cure residual strains through the thickness of carbon-epoxy laminates using FBGs, Part II: Technological specimen*, Composites: Part A, **40**: 1534–1544, 2009.

5. RAMAKRISHNAN M., RAJAN G., SEMENOVA Y., FARRELL G., *Overview of fiber optic sensor technologies for strain/temperature sensing applications in composite materials*, *Sensors*, **16**(1): 99, 2016.
6. GÜEMES J., PEREZ J.S., *Fiber optics sensors*, [in:] *New trends in structural health monitoring*, Springer, Vienna, Austria, pp. 265–316, 2013.
7. KIM B-S., BERNET N., SUNDERLAND P., MANSON J-A., *Numerical analysis of the dimensional stability of thermoplastic composites using a thermoviscoelastic approach*, *Journal of Composite Materials*, **36**(20): 2389–2403, 2002.
8. DONG C., *A parametric study on the process-induced deformation of composite T-stiffener structures*, *Composites: Part A*, **41**: 515–520, 2010.
9. DONG C., *Process-induced deformation of composite T-stiffener structures*, *Composite Structures*, **92**: 1614–1619, 2010.
10. DING A., LI S., WANG J., ZU L., *A three-dimensional thermo-viscoelastic analysis of process-induced residual stress in composite laminates*, *Composite Structures*, **129**: 60–69, 2015.
11. DING A., LI S., SUN J., WANG J., ZU L., *A thermo-viscoelastic model of process-induced residual stresses in composite structures with considering thermal dependence*, *Composite Structures*, **136**: 34–43, 2016.
12. CLIFFORD S., JANSSON N., YU W., MICHAUD V., MANSON J-A., *Thermoviscoelastic anisotropic analysis of process induced residual stresses and dimensional stability in real polymer matrix composite components*, *Composites: Part A*, **37**: 538–545, 2006.
13. LI J., YAO X., LIU Y., CEN Z., KOU Z., HU X., DAI D., *Thermo-viscoelastic analysis of the integrated T-shaped composite structures*, *Composites Science and Technology*, **70**: 1497–1503, 2010.
14. FERRY J., *Viscoelastic properties of polymers*, John Wiley & Sons, 1980.
15. SCHWARZL F., STRUIK L., *Analysis of relaxation measurements*, *Advances in Molecular Relaxation Processes*, **1**: 201–255, 1967.
16. ZOBEIRY N., VAZIRI R., POURSARTIP A., *Computationally efficient pseudo-viscoelastic models for evaluation of residual stresses in thermoset polymer composites during cure*, *Composites: Part A*, **41**: 247–256, 2010.
17. ADOLF D., MARTIN J., *Calculation of stress in crosslinking polymers*, *Journal of Composite Materials*, **30**(1): 13–34, 1996.
18. JOHNSTON A., *An integrated model of the development of process-induced deformation in autoclave processing of composite structures*, PhD Thesis, University of British Columbia, 1997.
19. *Standard test method for glass transition temperature (DMA T_g) of polymer matrix composites by dynamic mechanical analysis (DMA)*, ASTM International D 7028, 2007.
20. LAKES R., *Viscoelastic materials*, Cambridge University Press, New York 2009.
21. ALBERT C., FERNLUND G., *Spring-in and warpage of angled composite laminates*, *Composites Science and Technology*, **62**: 1895–1912, 2002.
22. RADFORD D., RENNICK T., *Separating sources of manufacturing distortion in laminated composites*, *Journal of Reinforced Plastics and Composites*, **19**: 621–641, 2000.

23. KIM Y., *Process-induced viscoelastic residual stress analysis of graphite-epoxy composite structures*, PhD Thesis, University of Illinois at Urbana-Champaign, 1996.
24. LI C., POTTER K., WISNOM M., STRINGER G., *In-situ measurement of chemical shrinkage of MY750 epoxy resin by a novel gravimetric method*, Composites Science and Technology, **64**: 55–64, 2004.
25. GALIŃSKA A., *Material models used to predict spring-in of composite elements: a comparative study*, Applied Composite Materials, **24**(1): 159–170, 2017.
26. BARBERO E., *Finite element analysis of composite materials*, CRC Press, Taylor & Francis Group, Department of Mechanical and Aerospace Engineering, West Virginia University, USA, 2008.
27. MOTTAHEDI M., DADALAU A., HAFLA A., VERL A., *Numerical analysis of relaxation test based on Prony series material model*, Stuttgart Research Centre for Simulation Technology (SRC Sim Tech), 1, 2009.

Received April 18, 2017; accepted version February 21, 2018.
